Warm storage for arc magmas

Mélanie Barboni[a,1], Patrick Boehnke[a], Axel K. Schmitt[b], T. Mark Harrison[a,1], Phil Shane[c], Anne-Sophie Bouvier[d], and Lukas Baumgartner[d]

[a]Department of Earth, Planetary, and Space Sciences, University of California, Los Angeles, CA 90095; [b]Institute of Earth Sciences, Heidelberg University, 69120 Heidelberg, Germany; [c]School of Environment, The University of Auckland, 1142 Auckland, New Zealand; and [d]Institute of Earth Sciences, University of Lausanne, 1015 Lausanne, Switzerland

Contributed by T. Mark Harrison, September 28, 2016 (sent for review August 2, 2016; reviewed by George Bergantz and Jonathan Miller)

Felsic magmatic systems represent the vast majority of volcanic activity that poses a threat to human life. The tempo and magnitude of these eruptions depends on the physical conditions under which magmas are retained within the crust. Recently the case has been made that volcanic reservoirs are rarely molten and only capable of eruption for durations as brief as 1,000 years following magma recharge. If the "cold storage" model is generally applicable, then geophysical detection of melt beneath volcanoes is likely a sign of imminent eruption. However, some arc volcanic centers have been active for tens of thousands of years and show evidence for the continual presence of melt. To address this seeming paradox, zircon geochronology and geochemistry from both the frozen lava and the cogenetic enclaves they host from the Soufrière Volcanic Center (SVC), a long-lived volcanic complex in the Lesser Antilles arc, were integrated to track the preeruptive thermal and chemical history of the magma reservoir. Our results show that the SVC reservoir was likely eruptible for periods of several tens of thousands of years or more with punctuated eruptions during these periods. These conclusions are consistent with results from other arc volcanic reservoirs and suggest that arc magmas are generally stored warm. Thus, the presence of intracrustal melt alone is insufficient as an indicator of imminent eruption, but instead represents the normal state of magma storage underneath dormant volcanoes.

volcano | eruption | arc magma | zircon

Determining the timescale of magma storage and remobilization in the upper crust is key to understanding the tempo and magnitude of volcanic eruptions (1–13). Whether a volcano can erupt is controlled by the recharge rate to the magma reservoir (13) (reservoir in this context refers to the portion of the igneous complex that is potentially eruptible), which in turn determines the duration of the "eruption window" [generally defined as the rheological state during which the subvolcanic reservoir is below ~60% crystals and hence capable of eruption (4)]. However, estimates for how long this eruption window remains open vary over four orders of magnitude; this suggests either profound problems in assumptions underlying one or more of these estimates or a continuum of physical mechanisms that resist formulation of a unified model for the state of magma reservoirs before eruption (1–13). The preservation of sharp compositional gradients in plagioclase phenocrysts, assumed to have crystallized >10 ka before eruption, has recently been interpreted to indicate that arc volcanic reservoirs characteristically remain in "cold storage" at temperatures below the eruption window, possibly below the solidus, and thus only capable of erupting during brief recharge events (<10 ka) (1). In contrast, zircon dating and heat budget considerations are difficult to reconcile with this scenario; instead, they are consistent with continuously partially molten reservoirs capable of erupting (i.e., with melt portion ≥40%) over long durations (>>10 ka) (6–12). Whatever these differences, all agree that understanding the thermal history of the magmatic reservoir is key to constraining the duration of the eruption window (3, 12).

Coupling zircon microgeochronology and geochemistry provides powerful insights into the preeruptive evolution of volcanic centers (14, 15), but thus far this approach has been applied either to volcanic or plutonic end-members. That intrusive magma volumes outweigh their extrusive counterparts is sufficient reason to assume that both may record different aspects of the reservoir's history (15–19); this is because melt-dominated volcanic rocks may only represent a volumetrically minor part of the magma reservoir, whereas plutonic rocks represent conditions in the crystal-dominated bulk of the magma reservoir (18). To provide a physical context for our interpretive scheme, we point to simulations of Bergantz et al. (19) that show that the full extent of thermal excursions caused by recharge is only recorded in the immediately adjacent crystal-rich portions of the reservoir.

In this paper, we integrate high spatial-resolution U-series ages of zircon coupled with trace element geochemistry of both the extrusive dacite and cogenetic enclaves (Fig. S1). The enclaves from the Quaternary Soufrière Volcanic Center (SVC), Saint Lucia, Lesser Antilles (Fig. 1), studied here are remarkable in the level of detailed petrologic investigation they have experienced by previous researchers (20, 21). We focus on zircon rims to avoid any inherited cores, but note that due to the continuous growth of zircon and limited depth resolution of secondary ion mass spectrometer (SIMS) U-Th dating, our ages average over the outer ~4 μm of each zircon.

SIMS U-Th zircon geochronology and trace element analysis of zircon (*SI Text*) were undertaken for a suite of SVC enclaves, yielding crystallization ages up to 130 ka (Fig. 2 and Figs. S1–S3; Datasets S1 and S2; sample description in *SI Text*), and the host lava of the Belfond Dome, which erupted at 13.6 ± 0.4 ka (21) (Fig. 1). Ti contents of zircons in cogenetic enclaves show spikes in crystallization temperatures (Ti-in-zircon) (22, 23) (see *SI Text*, Fig. S4, and Dataset S3 for methodology and discussion

Significance

The increasingly popular notion that steady-state magma chambers are highly crystallized, and thus only capable of erupting during brief (<1 ka) reheatings, implies that melt detection beneath volcanoes warns of imminent eruption. By integrating the microgeochronology and geochemistry of zircons from lavas with those from components crystallized within the magma chamber and incorporated during eruption, we show that the Soufrière (Saint Lucia) volcanic reservoir was instead eruptible over long (>100 ka) timescales. Together with data from other volcanic complexes, we show that arc magmas may generally be stored warm (are able to erupt for >100 ka). Thus geophysical detection of melt beneath volcanoes represents the normal state of magma storage and holds little potential as an indicator of volcanic hazard.

Author contributions: M.B., A.K.S., and T.M.H. designed research; M.B., P.B., A.K.S., P.S., A.-S.B., and L.B. performed research; M.B., P.B., A.K.S., and T.M.H. analyzed data; and M.B., P.B., A.K.S., T.M.H., P.S., A.-S.B., and L.B. wrote the paper.

Reviewers: G.B., University of Washington; and J.M., San Jose State University.

The authors declare no conflict of interest.

[1]To whom correspondence may be addressed. Email: tmark.harrison@gmail.com or mbarboni@epss.ucla.edu.

This article contains supporting information online at www.pnas.org/lookup/suppl/doi:10.1073/pnas.1616129113/-/DCSupplemental.

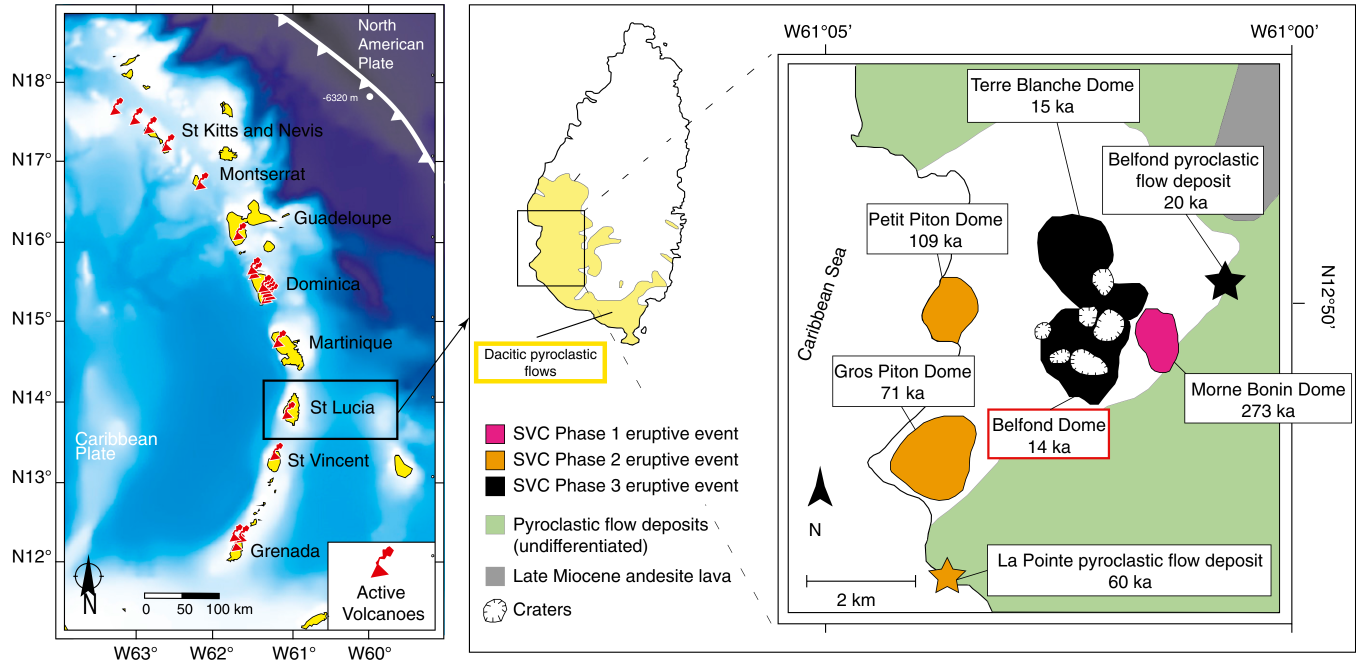

Fig. 1. (*Left*) Location of Saint Lucia in the Lesser Antilles with positions of active volcanoes within the arc; shades of blue relate to bathymetry (darker indicates deeper). (*Right*) Geological sketch map of the SVC with main eruptive phases and (U-Th/He) eruption ages (21). Stars represent sampling locations of pyroclastic flow deposits that are related to the SVC eruption phases (see color coding) and whose eruption was dated by (U-Th)/He zircon methods (21).

regarding a_{TiO2}) that coincide with the main eruption phases recorded in the SVC (phase 2 and 3; Figs. 1 and 2*A*). These spikes are interpreted as resulting from recharge of juvenile magma into the magma reservoir. We estimate a lower bound for the maximum temperature reached during the recharge event from the highest calculated value of 880 ± 20 °C (Fig. 2*A*), which would dissolve most of the preexisting plagioclase and quartz (24). Indeed, the subdued Eu/Eu* in the enclave zircon likely records the release of Eu^{2+} back into the melt (Fig. 2*B*) due to near-complete resorption of plagioclase. Because quartz and plagioclase are >40% of the mineral assemblage of the cogenetic enclaves (which at the typically lower temperatures recorded outside the spike intervals would be a crystal mush) (*SI Text*), the prograde thermal excursion locally reduced the proportion of crystals below 60% and thus placed at least part of the reservoir into the eruption window.

The overall longevity of the SVC magma reservoir is supported by the abundance of zircons extracted from the lava that show an extended and continuous period of crystallization spanning ∼250 ka (Fig. 2 and Dataset S2). In contrast to the plutonic zircons, the volcanic zircons do not exhibit any resolved spikes in temperature or Eu/Eu*, instead showing a constant decrease in Eu/Eu*, suggesting continuous plagioclase fractionation throughout their history (Fig. 2*B*). These results show that the ultimately erupted part of the magma reservoir beneath the SVC remained above its solidus (∼700 °C at 1–2 kbar; ref. 25; reservoir depth estimation following geophysical model from other volcanoes in the Caribbean arc from ref. 26) over at least the last 140 ka and likely back to 250 ka (Figs. 1 and 2). This contrasting behavior recorded by the lava and enclave zircons is best reconciled by the latter forming during cooling from a heating event associated with recharge by juvenile magma. The lack of temperature spikes in the volcanic zircons requires that that portion of the reservoir having remained above the solidus between rejuvenation events was of sufficient size that such recharge events did not affect the entire reservoir, but only its proximal surroundings. The evidence is consistent with the view that cogenetic enclaves reflect individual recharge events that heated only parts of the reservoir, whereas the volcanic zircons are derived from a thermally buffered reservoir that continuously retained melt. That is, the lava only experienced the recharge event that led to its removal from the reservoir. Our inference is consistent with simulations that show that the effects from recharge are likely to only be recorded in the crystal-rich part of the reservoir (19). The fact that older zircon rims are preserved throughout the magmatic history suggests that they were armored by (*i*) modal mineral phases or (*ii*) younger, subsequently resorbed rims, or that the melt-present part of the magma reservoir waxed and waned, permitting incorporation of some crystals from intermittently solidified margins before eruption (Fig. S1). Both components of the magma reservoir were sampled during the Belfond Dome eruption with most volcanic zircons crystallizing at steady state in supersolidus storage conditions, whereas enclave zircon crystallized during or immediately after transient rejuvenation from magma recharge. The coinciding trace elemental spikes in plutonic zircon and SVC eruption ages suggest to us a link between recharge and eruption. We note that zircon crystals from some cogenetic enclaves display correlated spikes in Ti-in-zircon temperature and Eu/Eu* (e.g., Gran 1.1, 1.4c, or 1.4d), whereas others do not (e.g., SLJL52; Fig. 3*A*), likely because zircon stability is a function of zirconium abundance [Zr], melt chemistry, and temperature (27, 28), and some cogenetic enclaves may not have saturated zircon at a sufficiently high temperature to record the spike. Indeed, we find a correlation between the magnitude of the temperature spike and the enclave [Zr] (Fig. 3*B*), illustrating that only the Zr-rich enclaves record the temperature excursion. The coupled geochemical and geochronological data from the SVC cogenetic enclaves provide the first direct constraints for remelting of a partially crystallized reservoir (crystal mush) (4, 29).

To constrain the minimum duration of the temperature spikes, we use the three cogenetic enclaves (Gran 1.1, 1.4d, and 1.10; Fig. 2) that record a well-defined excursion in Ti abundance and Eu/Eu* before the Belfond Dome eruption (13.6 ± 0.4 ka) (21). Using our zircon age and geochemistry data and the independently

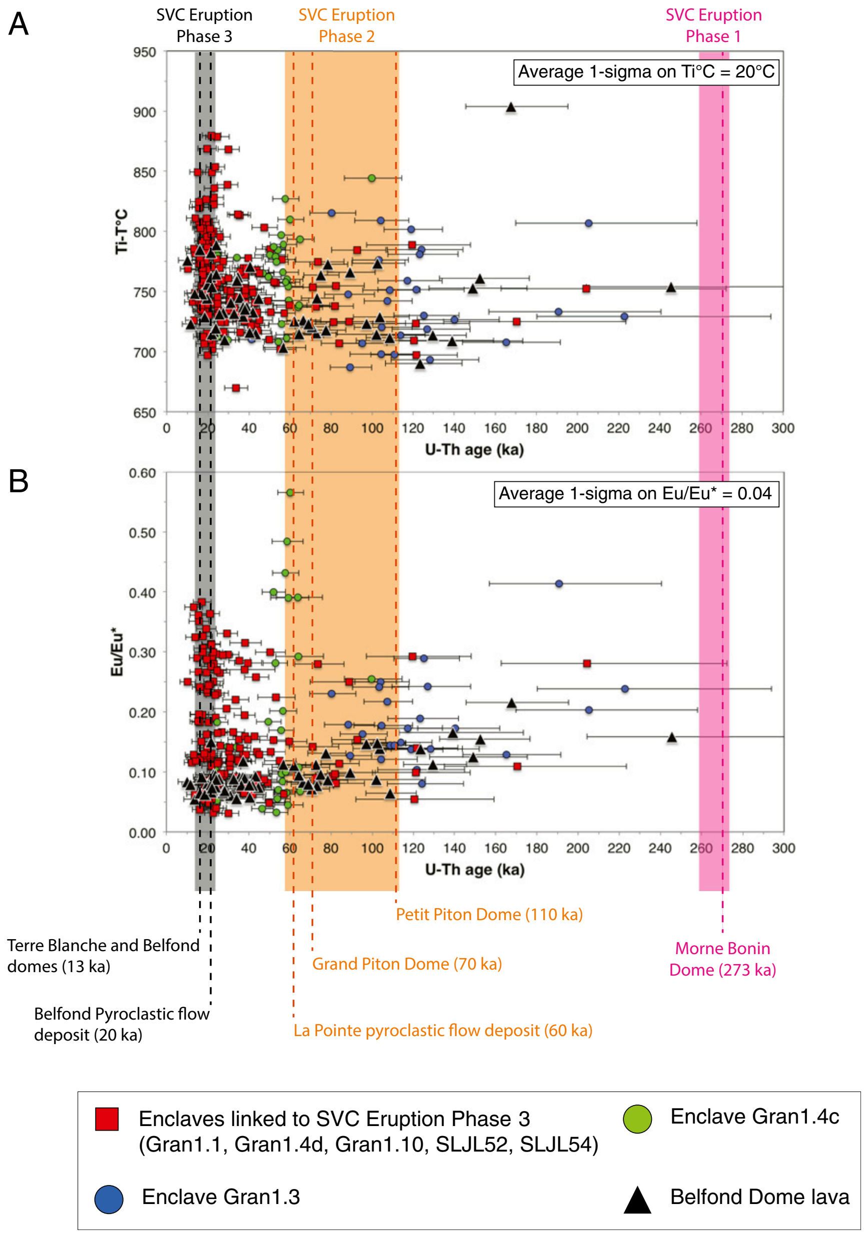

Fig. 2. Zircon U-Th model ages (in ka) vs. Ti-in zircon temperatures (*A*) and Eu/Eu* (determined using the geometric mean) (*B*) for the cogenetic enclaves and the Belfond lava, with main SVC eruptive phases and (U-Th)/He eruption ages (21). Errors are 1σ.

known eruption age, we calculate a duration of 14 ± 2 ka for the cooling following the magma recharge before the Belfond Dome eruption (Fig. 4 and *SI Text*). This time interval also encompasses an eruption at ~20 ka, which formed the extensive pyroclastic flow deposits of the Belfond unit covering a large portion of southwestern Saint Lucia (21). We note that the duration calculated here represents the amount of time that the reservoir spends in the eruption window during the cooling that follows from the recharge event, and is the minimum estimate because cooling following the thermal spike was interrupted by the Belfond Dome eruption. Furthermore, zircon saturation (and hence zircon crystallization) was only reached during cooling following the rejuvenation, and therefore our data can only constrain a lower bound on the duration of magma remobilization, because any increase in temperature immediately raises the [Zr] required for saturation and thus zircon tends to become unstable during heating. Results from other volcanic centers suggest that the rejuvenation itself could occur on a very short timescale (<1 y) (30). Our data are also best explained by the occurrence of a single, robust thermal spike (≥880 °C) rather than multiple heating episodes occurring on timescales that cannot be resolved by our zircon dates. In a multiple-spike model, the reservoir would have tended to dissolve zircon after each recharge, and thus the last rim would have crystallized just before, and not 15 ka before, eruption. The lower abundance of older enclave zircons supports the contention that recharge events destroyed earlier generations. That is to say, the cogenetic enclave population is likely biased toward younger ages because preexisting crystal-rich domains may become mixed into and assimilated by the magma or, alternatively, growth of new rims may obscure any previously recorded spikes. Zircon data from two of the studied enclaves also provide evidence for reservoir rejuvenations before the last spike. Enclave 1.4c contains zircons dating back to the reservoir reactivation during SVC eruption phase 2, with a spike defined by temperature and Eu/Eu* at ~60 ka (Fig. 2 and Dataset S2). By

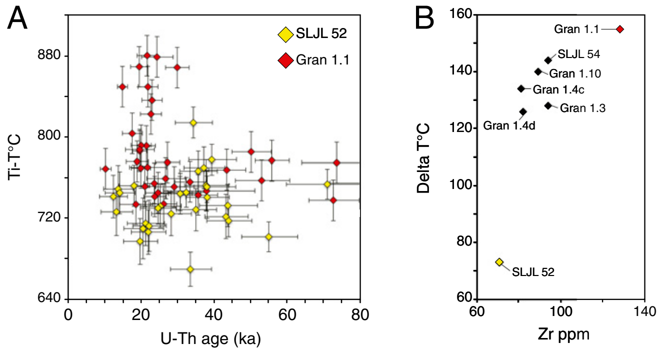

Fig. 3. (*A*) Zircon U-Th model ages (ka) vs. Ti-in zircon temperatures for cogenetic enclaves Gran 1.1 (spike recorded) and SLJL52 (no spike recorded). (*B*) Correlation between the extent of spike recorded and Zr whole rock abundance (δT °C is maximum − minimum temperature recorded in each enclave).

examining the range in zircon ages from 1.4c, we estimate a spike duration ranging from 20 to 40 ka for phase 2 (Fig. 2). The fact that many zircon crystals in enclave 1.4c postdate the SVC eruption phase 2 may reflect an incomplete chronostratigraphy for the SVC with not all eruptions being identified or dated. Enclave 1.3 contains even older zircons with a spike between 90 and 130 ka that may be related to the onset of the penultimate eruptive phase of the SVC (phase 2 in ref. 21) (Fig. 2 and Dataset S2). Additionally, we note that our calculated eruption window durations agree well with independently constrained cooling and crystallization timescales for the shallow-level calc-alkaline Elba Island pluton, where U-Pb zircon dating and thermal modeling indicated that rhyolitic magma remained at conditions conducive for eruptive melt extraction over ∼10–40 ka (6, 7).

The eruption windows for the SVC, as determined using combined zircon geochronology and geochemistry (from ∼15 up to ∼40 ka), are more protracted than those proposed using diffusion profile modeling of compositional gradients in plagioclase from arc volcanic reservoirs (i.e., ≤10 ka) (1). However, studies using diffusion profiles cannot assign crystallization ages to individual plagioclase crystal because current U-Th disequilibrium dating techniques requires multigrain aliquots (up to several grams) (1). Therefore, it cannot be ruled out that those crystals exhibiting disequilibrium profiles formed immediately before eruption. That is to say, apparent diffusion profiles more likely reflect the individual plagioclase crystal formation age rather than storage conditions. Relating bulk plagioclase U-Th ages to diffusion profiles in individual crystals requires that they formed simultaneously, a requirement that is unlikely to be met in magmatic reservoirs. Support for this hypothesis comes from Sr profiles in plagioclase from Kameni Island (Greece) and Soufrière (Saint Vincent) (31), where some are in equilibrium and others show apparent diffusion profiles. If interpreted to reflect storage conditions, the magma would simultaneously be stored cold and warm, whereas the alternative proposal that plagioclase crystallizes continuously does not result in such an internally inconsistent interpretation. This recognition effectively precludes using diffusion modeling of modal minerals to infer storage durations.

Based on (U-Th)/He zircon dating, the SVC experienced at least five eruptions during the last 120 ka (21) (Figs. 1 and 2). Combining the requirement from the mush model (4) that each eruption is linked to at least one recharge with zircon age and trace element constraints for eruption windows lasting 15–40 ka, we conclude that parts of the SVC reservoir remained within the eruption window for at least 120 ka. Further support for this inference comes from the continuous zircon crystallization and plagioclase fractionation in the volcanic host of the cogenetic enclaves (Fig. 2), which contradicts cold-storage models (1) for which calculated temperatures are <700 °C and hence below the solidus (*SI Text*). Additional support for our preferred scenario of continuous magma presence in the thermally buffered zone from which volcanic zircons are derived comes from Ti-in-zircon data from the Tarawera arc-volcano (New Zealand) where volcanic zircons crystallized continuously over 150 ka and show little resolvable variation in their crystallization temperatures (14).

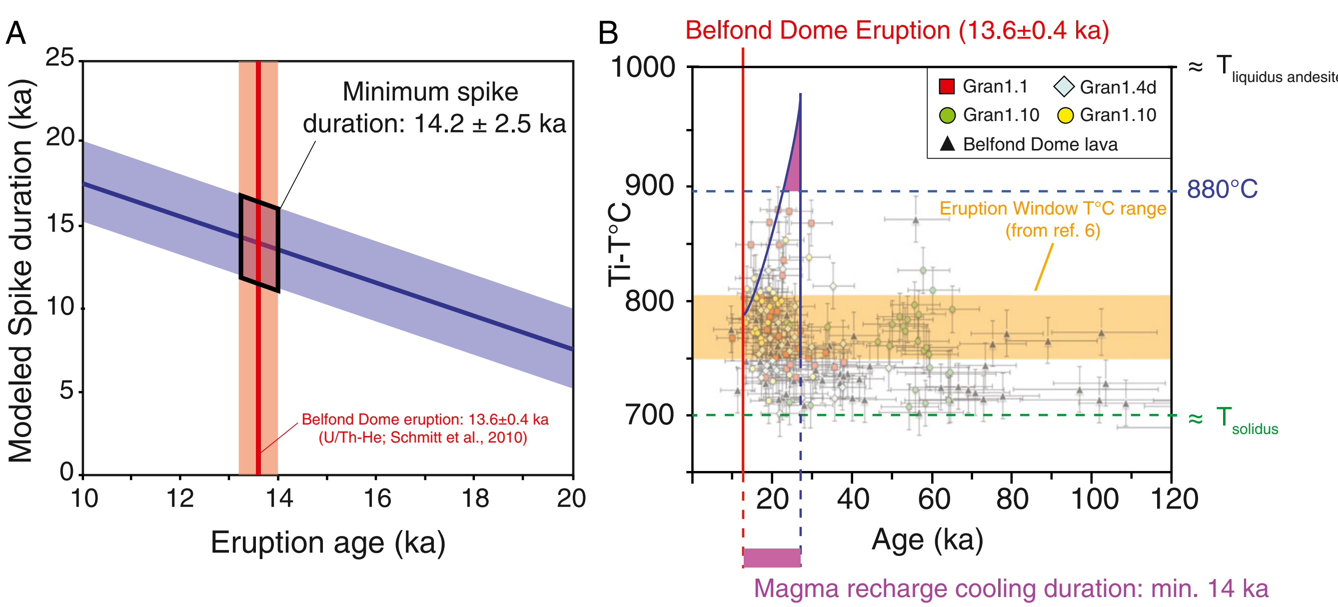

Fig. 4. (*A*) Minimum modeled spike duration constrained by the Belfond Dome eruption. Errors on modeled spike duration are 2σ. (*B*) Summary of mush rejuvenation events recorded by zircon U-Th model ages and Ti-in zircon temperatures within selected cogenetic enclaves and Belfond Dome lava. Errors are 1σ. Mush rejuvenation duration from our model. $T_{solidus}$ estimated by the lowest Ti-in zircon temperature from the zircon in the lava. $T_{liquidus\ andesite}$ from ref. 35. Minimum spike temperature estimated by the highest Ti-in zircon temperature from the cogenetic enclaves.

We conclude that eruptible magma reservoirs are generally long-lived (>100 ka), can continuously retain significant amounts of melt (<60% crystal fraction), and are stored broadly isothermally for timescales of tens to hundreds of thousands of years such that they can be rapidly mobilized and erupt. Volatiles liberated by hydrous magma recharge during decompression aid in rejuvenating the crystal mush by triggering the remelting process and facilitating eruption by decreasing melt viscosity (32).

The consistency of observations from two volcanic centers (Saint Lucia and Tarawera) and a shallow level plutonic reservoir (Elba) suggests our observation may be broadly applicable to other arc volcanoes of similar size and composition (e.g., Mount Saint Helens, Mount Pinatubo) (33, 34). Because the vast majority of modern continental volcanism is related to arcs, these findings have general implications for volcanic hazard assessments. Previous studies proposed that because magma chambers are ephemeral, detection of intracrustal melt might be a sign of imminent eruption (1). However, protracted crystallization ages and contrasting chemical variations in zircon from cogenetic volcanic and plutonic rocks call for the magma reservoir beneath the SVC being kept in warm storage (i.e., above the solidus, with portions residing continuously in the eruption window). Thermal energy considerations (3, 10, 12, 13) require a high rate of rejuvenation that leads to thermal excursions with durations >10 ka. Therefore, geophysical detection of melt beneath a volcano may hold little value as an indicator of volcanic hazards (1). By contrast, the extended use of the method applied in this study (U-Th ages combined with trace element on zircon from cogenetic volcanic and plutonic rocks) can provide superior insights into magma chamber evolution in potentially hazardous arc volcanoes based on absolute timescales.

Methods Summary

U-Th zircon analyses were performed on the University of California, Los Angeles (UCLA) CAMECA *ims*1270 and the Heidelberg University CAMECA *ims*1280-HR SIMS using the protocol described in ref. 36. Zircon trace elements abundances were acquired using the UCLA CAMECA *ims*1270, the Heidelberg University CAMECA *ims*1280-HR, and the Lausanne University CAMECA *ims*1280-HR (Swiss SIMS) ion probes following the analytical procedure described in ref. 37. U-Th and trace element analyses were made on the same spot on the zircon uppermost rim (crater average depth is ~4 μm). Description of the samples, SIMS protocol, Ti-in-zircon thermometry constraints, details on the spike duration modeling, and additional information on the Sr diffusion model of ref. 1 are given in *SI Text*.

ACKNOWLEDGMENTS. We thank Jan Lindsay for assistance in the field, Calvin Miller for his insightful comments, and George Bergantz and Jonathan Miller for their thoughtful reviews. We acknowledge Kari Cooper, Tim Druit, and two anonymous reviewers for their comments on a previous version of the manuscript. Support was obtained from The Swiss National Science Foundation (SNF) Grant P300P2_147740 (to M.B). The ion microprobe facility at UCLA is partly supported by a grant from the NSF Earth Sciences Instrumentation and Facilities Program. The SWISS-SIMS is supported by a grant from Bundesamt für Foschung und Innovation (Grant PCI-KIP 6 CASA to L.B.). The Heidelberg Ion Probe (HIP) facility at Heidelberg University is operated under the auspices of the DFG Scientific Instrumentation and Information Technology program. Support for fieldwork was obtained from a Performance Based Research Fund (PBRF) grant from the University of Auckland (to P.S.).

1. Cooper KM, Kent AJ (2014) Rapid remobilization of magmatic crystals kept in cold storage. *Nature* 506(7489):480–483.
2. Reid MR (2008) How long does it take to supersize an eruption? *Elements* 4:23–28.
3. Schöpa A, Annen C (2013) The effects of magma flux variations on the formation and lifetime of large silicic magma chambers. *J Geophys Res* 118:926–942.
4. Burgisser A, Bergantz GW (2011) A rapid mechanism to remobilize and homogenize highly crystalline magma bodies. *Nature* 471(7337):212–215.
5. Bachmann O, Bergantz GW (2008) Rhyolites and their source mushes across tectonic settings. *J Petrol* 49:2277–2285.
6. Barboni M, Schoene B (2014) Short eruption window revealed by absolute crystal growth rates in a granitic magma. *Nat Geosci* 7:524–528.
7. Barboni M, Annen C, Schoene B (2015) Evaluating the construction and evolution of upper crustal magma reservoirs with coupled U/Pb zircon geochronology and thermal modeling: A case study from the Mt. Capanne pluton (Elba, Italy). *Earth Planet Sci Lett* 432:436–448.
8. Gelman SE, Gutierrez FJ, Bachmann O (2013) On the longevity of large upper crustal silicic magma reservoirs. *Geology* 41:759–762.
9. Huber C, Bachmann O, Dufek J (2012) Crystal-poor versus crystal-rich ignimbrites: A competition between stirring and reactivation. *Geology* 40:115–118.
10. Annen C (2009) From plutons to magma chambers: Thermal constraints on the accumulation of eruptible silicic magma in the upper crust. *Earth Planet Sci Lett* 284: 409–416.
11. Costa F, Dohmen R, Chakraborty S (2008) Time scales of magmatic processes from modeling the zoning patterns of crystals. *Rev Mineral Geochem* 69:545–594.
12. Annen C (2011) Implications of incremental emplacement of magma bodies for magma differentiation, thermal aureole dimensions and plutonism–volcanism relationships. *Tectonophysics* 500:3–10.
13. Tierney CR, Schmitt AK, Lovera OM, de Silva SL (2016) Voluminous plutonism during volcanic quiescence revealed by thermochemical modeling of zircon. *Geology* 44: 683–686.
14. Storm S, Schmitt AK, Shane P, Lindsay JM (2014) Zircon trace element chemistry at sub-micrometer resolution for Tarawera volcano, New Zealand, and implications for rhyolite magma evolution. *Contrib Mineral Petrol* 167:1–19.
15. Deering CD, et al. (2016) Zircon record of the plutonic-volcanic connection and protracted rhyolite melt evolution. *Geology* 44:267–270.
16. Deering CD, Bachmann O (2010) Trace element indicators of crystal accumulation in silicic igneous rocks. *Earth Planet Sci Lett* 297:324–331.
17. Bachmann O, Miller C, de Silva S (2007) The volcanic–plutonic connection as a stage for understanding crustal magmatism. *J Volcanol Geotherm Res* 167:1–23.
18. Gelman SE, Deering CD, Bachmann O, Huber C, Gutiérrez FJ (2014) Identifying the crystal graveyards remaining after large silicic eruptions. *Earth Planet Sci Lett* 403: 299–306.
19. Bergantz GW, Schleicher JM, Burgisser A (2015) Open-system dynamics and mixing in magma mushes. *Nat Geosci* 8:793–796.
20. Arculus RJ, Wills KJ (1980) The petrology of plutonic blocks and inclusions from the Lesser Antilles island arc. *J Petrol* 21:743–799.
21. Schmitt AK, et al. (2010) Episodic growth and homogenization of plutonic roots in arc volcanoes from combined U–Th and (U–Th)/He zircon dating. *Earth Planet Sci Lett* 295:91–103.
22. Watson EB, Harrison TM (2005) Zircon thermometer reveals minimum melting conditions on earliest Earth. *Science* 308(5723):841–844.
23. Ferry JM, Watson EB (2007) New thermodynamic models and revised calibrations for the Ti-in-zircon and Zr-in-rutile thermometers. *Contrib Mineral Petrol* 154:429–437.
24. Naney MT (1983) Phase equilibria of rock-forming ferromagnesian silicates in granitic systems. *Am J Sci* 283:993–1033.
25. Lambert IB, Wyllie PJ (1972) Melting of gabbro (quartz eclogite) with excess water to 35 kilobars, with geological applications. *J Geol* 80(6):693–708.
26. Annen C, Pichavant M, Bachmann O, Burgisser A (2008) Conditions for the growth of a long-lived shallow crustal magma chamber below Mount Pelee volcano (Martinique, Lesser Antilles Arc). *J Geophys Res Solid Earth*, 10.1029/2007JB005049.
27. Watson EB, Harrison TM (1983) Zircon saturation revisited: Temperature and composition effects in a variety of crustal magma types. *Earth Planet Sci Lett* 64:295–304.
28. Boehnke P, Watson EB, Trail D, Harrison TM, Schmitt AK (2013) Zircon saturation re-revisited. *Chem Geol* 351:324–334.
29. Bachmann O, Bergantz GW (2004) On the origin of crystal-poor rhyolites: Extracted from batholithic crystal mushes. *J Petrol* 45:1565–1582.
30. Gualda GAR, Sutton SR (2016) The year leading to a supereruption. *PLoS One* 11(7): e0159200.
31. Zellmer GF, Blake S, Vance D, Hawkesworth C, Turner S (1999) Plagioclase residence times at two island arc volcanoes (Kameni Islands, Santorini, and Soufriere, St. Vincent) determined by Sr diffusion systematics. *Contrib Mineral Petrol* 136:345–357.
32. Huber C, Bachmann O, Manga M (2009) Homogenization processes in silicic magma chambers by stirring and mushification (latent heat buffering). *Earth Planet Sci Lett* 283:38–47.
33. Tilling RI (1984) *Eruptions of the Mount St. Helens: Past, Present, and Future* (US Geological Survey, Reston, VA).
34. Wolfe EW, Hoblitt RP (1996) *Fire and Mud: Eruptions and Lahars of Mount Pinatubo, Philippines*, eds Newhall CG, Punongbayan, RS (Philippine Institute of Volcanology and Seismology, Quezon City, Philippines/Univ of Washington Press, Seattle), pp 751–766.
35. Alonso-Perez R, Müntener O, Ulmer P (2009) Igneous garnet and amphibole fractionation in the roots of island arcs: Experimental constraints on andesitic liquids. *Contrib Mineral Petrol* 157:541–558.
36. Schmitt AK, Stockli DF, Hausback BP (2006) Eruption and magma crystallization ages of Las Tres Virgenes (Baja California) constrained by combined 230Th/238U and (U-Th)/He dating of zircon. *J Volcanol Geotherm Res* 158:281–295.
37. Storm S, Shane P, Schmitt AK, Lindsay JM (2011) Contrasting punctuated zircon growth in two syn-erupted rhyolite magmas from Tarawera volcano: Insights to crystal diversity in magmatic systems. *Earth Planet Sci Lett* 301:511–520.
38. Lindsay JM, et al. (2013) Volcanic stratigraphy and geochemistry of the Soufrière Volcanic Centre, Saint Lucia with implications for volcanic hazards. *J Volcanol Geotherm Res* 258:126–142.
39. Paces JB, Miller JD (1993) Precise U-Pb ages of Duluth complex and related mafic intrusions, northeastern Minnesota: Geochronological insights to physical,

petrogenetic, paleomagnetic, and tectonomagmatic processes associated with the 1.1 Ga midcontinent rift system. *J Geophys Res* 98:13997–14013.
40. Turner S, et al. (1996) U- series isotopes and destructive plate margin magma genesis in the Lesser Antilles. *Earth Planet Sci Lett* 142:191–207.
41. Boehnke P, Barboni M, Bell EA (2016) Zircon U/Th model ages in the presence of melt heterogeneity. *Quat Geochronol* 34:69–74.
42. Luo Y, Ayers JC (2009) Experimental measurements of zircon/melt trace-element partition coefficients. *Geochim Cosmochim Acta* 73:3656–3679.
43. Wright HM, et al. (2015) Episodic Holocene eruption of the Salton Buttes rhyolites, California, from paleomagnetic, U-Th, and Ar/Ar dating. *Geochem Geophys Geosyst* 16:1198–1210.
44. Stelten ME, Cooper KM, Vazquez JA, Calvert AT, Glessner JJ (2015) Mechanisms and timescales of generating eruptible rhyolitic magmas at Yellowstone caldera from zircon and sanidine geochronology and geochemistry. *J Petrol* 56:1607–1642.
45. Bell EA, Boehnke P, Harrison TM (2016) Recovering the primary geochemistry of Jack Hills zircons through quantitative estimates of chemical alteration. *Geochim Cosmochim Acta* 191:187–202.
46. Wark DA, Hildreth W, Spear FS, Cherniak DJ, Watson EB (2007) Pre-eruption recharge of the Bishop magma system. *Geology* 35:235–238.
47. Holland TJB, Powell R (1998) An internally consistent thermodynamic data set for phases of petrological interest. *J Metamorph Geol* 16:309–343.
48. Hayden LA, Watson EB (2007) Rutile saturation in hydrous siliceous melts and its bearing on Ti-thermometry of quartz and zircon. *Earth Planet Sci Lett* 258:561–568.
49. Efron B, Gong G (1983) A leisurely look at the bootstrap, the jackknife, and cross-validation. *Am Stat* 37:36–48.
50. Cherniak DJ, Watson EB (1994) A study of strontium diffusion in plagioclase using Rutherford backscattering spectroscopy. *Geochim Cosmochim Acta* 58:5179–5190.

Supporting Information

Barboni et al. 10.1073/pnas.1616129113

SI Text

Sample Petrology and Whole-Rock Geochemistry. Whole-rock major and trace elements are reported in Dataset S1, representative thin section pictures are presented in Fig. S1, and a selection of Harker diagrams is presented in Fig. S2.

Belfond Dome Lava (Sample SLJL25). Belfond Dome lava petrology and geochemistry were described in detail in ref. 38. The zircon crystals studied here come from a fresh dacitic clast within one of the Belfond Dome lava flow (67 wt% SiO_2; Dataset S1). This sample contains ~30% phenocrysts, 20% of which are plagioclase with minor quartz (5%), weathered biotite (3%), and minor amphibole and Fe-Ti oxides (2%) (Fig. S1). Together with several other compositionally identical Belfond Dome lava samples analyzed in ref. 38, this sample lacks evidence for major plagioclase fractionation in its whole-rock signature as shown by the relatively flat pattern (Eu/Eu* = 0.86) and no obvious depletion in Sr (310 ppm) contents (Fig. S2).

Plutonic Enclaves. The cogenetic plutonic enclaves found in the Belfond Dome lava vary in size (10–50 cm) and have subangular shapes (Fig. S1). Their composition varies from dioritic to granodioritic (54–60 wt% SiO_2) with a mineralogy dominated by amphibole (20–30%), plagioclase (25–35%), and quartz (20–30%), with minor biotite (<15%) and accessory minerals (Fe-Ti oxides, zircon, and apatite; Fig. S1). Most plagioclase in the enclaves show evidence for resorption and complex zoning in thin section (Fig. S1). Interstitial glass is minor (<3%).

Zircon U-Th Geochronology. Zircon separates were prepared by standard density and magnetic mineral separation methods (crushing and milling; sieving to <500 µm; concentration via hand-panning; magnetic separation; hand-picking). Zircons from both lava and enclaves typically had adherent glass that was removed by etching in 50% Hf for 1–2 min at room temperature (Fig. S3). Analyses were performed on unpolished crystal rim from zircon pressed into indium (In) metal. U-Th and trace element analyses were made on the same spot on the zircon uppermost rim (crater average depth is ~4 µm), as shown in Fig. S3.

U-Th analyses were performed on the University of California, Los Angeles (UCLA) CAMECA *ims*1270 and the Heidelberg University CAMECA *ims*1280-HR SIMS using a modified protocol from ref. 36, as described in ref. 37. U-Th relative sensitivities were calibrated from analysis of equilibrium zircon standard AS3 (1099.1 Ma) (39). Accuracy of background correction and relative sensitivity were checked by repeated measurements of AS3 in the course of the analysis. $(^{230}Th)/(^{238}U)$ values on the AS3 were 1.015 ± 0.006 [1σ; mean square weighted deviation (MSWD) = 1.7; n = 34] and 1.010 ± 0.012 (1σ; MSWD = 0.52; n = 10), within 1–2% of the expected ratio of unity and therefore within the typical reproducibility of the U-Th relative sensitivity calibration.

We calculated zircon model ages as two-point zircon-melt model isochrons, using the average of two Saint Lucia dacite whole-rock analyses with $(^{230}Th)/(^{232}Th) = 0.85 \pm 0.07$ and $(^{238}U)/(^{232}Th) = 0.72 \pm 0.12$ (40) (reported as method 1 ages in Dataset S2). However, this approach requires that the melt is chemically homogeneous and invariant in the production and loss of ^{230}Th. However, because we are considering both zircons from the lava and enclaves it is unlikely that the whole-rock analyses accurately capture both melt compositions. To test the importance of the assumption that all our zircons crystallize from a single melt composition, we implement an alternative age calculation method. Boehnke et al. (41) propose an age calculation using the fact that ratios of partition coefficients are unlikely to change with T or P variations (42) to calculate U-Th ages; they use the measured zircon U/Th to predict a U/Th of the melt based on $D_U/D_{Th} = 7 \pm 0.4$ (1σ) derived from zircon/melt inclusions pair (43, 44) and then the assumption that melts are within 15% (1σ) of the equiline based off data from continental volcanoes. The assumption of melts being near the equiline is derived from a compilation of whole rock and glass data that shows that most melts are near the equiline. Once the predicted melt value is calculated, a two-point isochrons is calculated using the measured zircon values. These model ages are reported as method 2 ages in Dataset S2. The agreement between the two methods suggests that compositional variability in the samples has little effect, and that the age calculations are robust.

Zircon Trace Elements Analysis. Zircon trace elements abundances were acquired using the UCLA CAMECA *ims*1270, the Heidelberg University CAMECA *ims*1280-HR, and the Lausanne University CAMECA *ims*1280-HR (Swiss SIMS) ion probes following the analytical procedure described in ref. 14. Trace elements on individual zircon rims (n = 276) are reported in Dataset S2.

Despite its chemically robust nature, zircon is susceptible to alteration and contamination in some instances. Contamination by nanoinclusions of other phases can affect the trace element content measured for zircon. Such compromised analyses are typically identified qualitatively by an increase in light rare-earth elements (LREEs), as well as P and other light elements (44), with the LREE a particularly good measure due to their rarity in primary crystalline zircon. The LREE alteration index (LREE AI) (44) is a measure of the degree of alteration based upon the shape of the REE pattern and is defined by

$$\text{LREE AI} = \frac{Dy}{Nd} + \frac{Dy}{Sm}.$$

High LREE AI indicates low LREE relative to the middle rare earth element (MREE) characteristic of unaltered zircon, whereas low LREE AI indicates likely beam overlap onto inclusions. Bell et al. (44) propose that samples with LREE AI > 30 have trace element contents dominated by primary magmatic processes, whereas those below 10 are dominated by alteration/contamination. We applied this index, together with the amount of Fe, Mg, and Mn (indicative of small oxide inclusions that can compromise our Ti measurements), to filter our dataset and identify contaminated analyses (Dataset S2).

[Ti] in Zircon Thermometry. Calculating absolute temperatures from [Ti] in zircon requires that we constrain the Si activity ($aSiO_2$) and Ti activity ($aTiO_2$) in the melt (23). The presence of quartz in all our samples constrains $aSiO_2 = 1$. Because rutile is not present in our sample, $aTiO_2$ is less than 1. We use two methods to constrain $aTiO_2$: the first one is to use the equilibrium between coexisting ilmenite and magnetite within the Terre Blanche lava (another late Pleistocene dacite dome in the SVC) (Dataset S3), following the procedure described in ref. 46 and using the relationships

$$2FeTiO_3 - Fe_2TiO_4 = TiO_2$$

and

$$K = \frac{a\mathrm{TiO_2}}{\left(a^{Ilm}_{\mathrm{FeTiO_3}}\right)^2 a^{Mag}_{\mathrm{Fe_2TiO_4}}}.$$

The values of the equilibrium constant were calculated from tabulated thermodynamic data from ref. 47 (Dataset S3), choosing as a standard state the pure phases ilmenite, ulvöspinel, and rutile at the temperatures and pressure of interest (765–825 °C; 1 bar). $a\mathrm{TiO_2}$ relative to pure rutile is then calculated from the composition of the coexisting magnetite and ilmenite (Dataset S3). Four pairs of oxides were measured (see Fig. S4 for one pair example), which yield $a\mathrm{TiO_2}$ values ranging between 0.31 and 0.38, with an average of 0.34 (Dataset S3).

The second way we determined $a\mathrm{TiO_2}$ is by calculating the [Ti] required for rutile saturation and to compare it to the [Ti] present in the SVC lava. We used the solubility equation from ref. 48, which the authors derived from experimental determinations of rutile saturation for felsic compositions.

$$\log(\mathrm{Ti,\ ppm}) = 7.95 - \frac{5305}{T(\mathrm{K})} + 0.124\mathrm{FM}$$

with

$$\mathrm{FM} = \frac{1}{Si}\frac{\mathrm{Na}+\mathrm{K}+2(\mathrm{Ca}+\mathrm{Mg}+\mathrm{Fe})}{Al}$$

from which $a\mathrm{TiO_2}$ can be derived using

$$a\mathrm{TiO_2} = \frac{\mathrm{Ti}^{\mathrm{sample}}_{\mathrm{measured}}}{\mathrm{Ti}^{\mathrm{sample}}_{\mathrm{saturation}}}.$$

Using the whole-rock composition from the Belfond lava (sample SLJL25) and the average temperature given by the [Ti] in zircon thermometer for this sample (747 °C; Dataset S2), we calculate $\mathrm{Ti_{saturation}}$ = 827 ppm and $a\mathrm{TiO_2}$ = 0.31 for the Belfond Dome lava. Both methods yield similar $a\mathrm{TiO_2}$, and we chose to use $a\mathrm{TiO_2}$ = 0.3 for our temperature calculation. We note that low $a\mathrm{TiO_2}$ is in line with the absence of titanite in our sample ($a\mathrm{TiO_2} <$ 0.6) and the presence of ilmenite as the only Ti-rich phase (minor Ti-magnetite is present). A different value for $a\mathrm{TiO_2}$ would not significantly affect the relative temperature variations. Changing $a\mathrm{TiO_2}$ from 0.3 to 0.6 would lower the minimum temperature reached in the reservoir during the rejuvenation event (as recorded by the highest [Ti] in zircon T°C; see main text) by ~80 °C (800 °C rather than 880 °C), but yields unrealistically low (subsolidus) minimum temperatures for zircon.

Modeling the Spike Duration. Zircons that are included in the spike width model for the event before the Belfond Dome eruption come from Enclaves 1.1, 1.4d, and 1.10. These zircon data were screened based on their geochemistry, including any zircon younger than the oldest zircon for which the Ti-in-zircon or Eu anomaly is resolved from the lava zircon. We then used the zircon ages and calculated the difference between the oldest zircon in the spike and our assumed eruption age. We varied the eruption age from 10 to 20 ka, and the resulting spike duration is a strong function of the eruption age (Fig. 4*A*). For our modeling we used bootstrap resampling (49) to propagate the age uncertainties and to resample our distribution of zircon ages. To further correct for the analytical uncertainty, the spike widths as shown were corrected for the expected variation in ages assuming MSWD = 1 and all errors are captured by the analytical uncertainty. Because we have 82 zircons in our spike, we expect that the oldest zircon could be 2.73σ older than the onset of the spike. Our correction therefore multiplies the analytical uncertainties of the oldest zircon in each resampling by 2.73 and subtracts that from the initially calculated spike duration. This correction reduces our inferred spike widths by ~16 ka. This duration is likely to underestimate the true spike widths as we have taken a conservative approach to uncertainty propagation. Additionally, because our criteria were used to remove zircons from the dataset, more data would only increase our inferred time interval. Using the U/Th age calculation based on published whole-rock composition for the SVC would increase the calculated spike duration by ~5 ka, and this is therefore a minimum width for the rejuvenation event that leads to the Belfond Dome eruption.

Sr Diffusion in Plagioclase. Cooper and Kent (1) argue that because Sr diffusion in plagioclase, which has a bulk age of >21 ka, shows a maximum residence time of either ~5.5 or 12 ka at 700 °C, the magma must have been in cold storage (below the lock-up temperature); however, they do not explicitly define the temperature of cold storage, providing only a hint that it might be below the solidus (figure 2 of ref. 1). Because Cooper and Kent's extended data table 1 in ref. 1 shows that 700 °C is too hot to explain the diffusion data, we extend their calculation to calculate a maximum storage temperature. Using experimentally determined coefficients for Sr diffusion in plagioclase (50), we use Cooper and Kent's (1) approach to calculate a maximum temperature of 685 °C at which the crystal could reside over the entire lifetime of 21 ka without significantly altering its Sr distribution. This calculation overestimates the actual storage temperature because it assumes that the entire profile was generated during storage, neglecting any diffusion during a high temperature spike. If indeed the majority of the diffusion happened during this spike (as envisioned by ref. 1), crystal storage temperatures would further decrease. For example, if 90% of the diffusion happened during the spike, then the maximum storage temperature would be 575 °C. Therefore, the maximum storage temperature is 685 °C. We reiterate that our examination of the data from ref. 1 is taking the authors' exact interpretation, and we are providing only a temperature for what they term as cold storage.

Having calculated a cold-storage temperature, we note that it is incompatible with our zircon data. The interpretation of ref. 1 that magmas are usually below the lock-up temperature stems from the claim that the timescale estimated from Sr diffusion profiles must be equal to the U-Th ages. However, to determine the U-Th ages, Cooper and Kent (1) analyzed bulk plagioclase, whereas the diffusion profiles were measured for individual crystals; this leads us to an alternate interpretation for the data of ref. 1, that is, the bulk of the plagioclase is old and contains no visible diffusion profiles with a few rare plagioclases crystallizing close to eruption. For example, plagioclase crystals from Kameni Island and Saint Vincent are either in equilibrium or not in equilibrium depending on the crystal (31), supporting our contention that the bulk of the plagioclase crystallizes early with only a minor population crystallizing just before eruption. Therefore, because it is not possible to relate diffusion profiles in a single crystal to U-Th ages from bulk plagioclase, there is no reason these timescales should agree, and to relate Sr diffusion in plagioclase to U-Th ages, the same crystal must be analyzed for both. Therefore, the data from ref. 1 cannot be uniquely used to infer cold storage of magmas at either below the lock-up temperature or, as required by the authors' data, the solidus.

Fig. S1. Thin sections of the lava and enclave samples, with example of enclave as found in the Belfond lava.

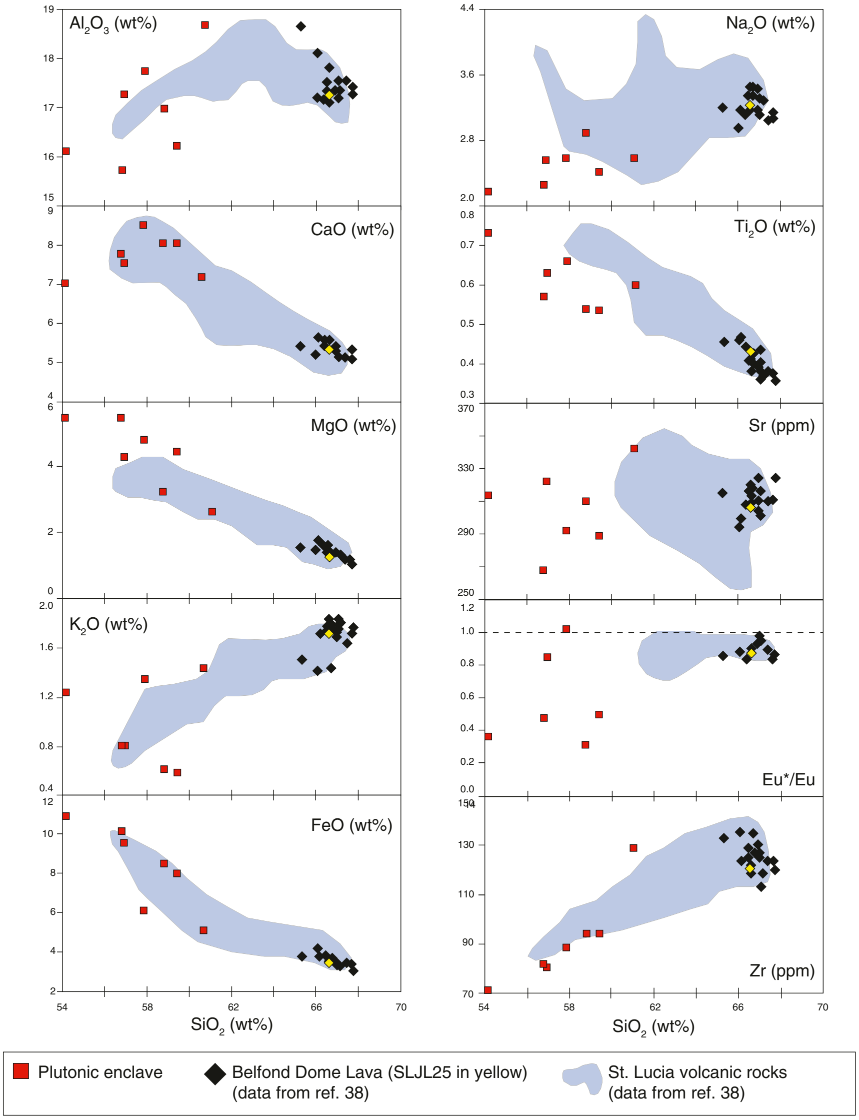

Fig. S2. Harker diagrams of selected major and trace elements for the plutonic enclaves, Belfond lava, and other volcanic rocks from Saint Lucia.

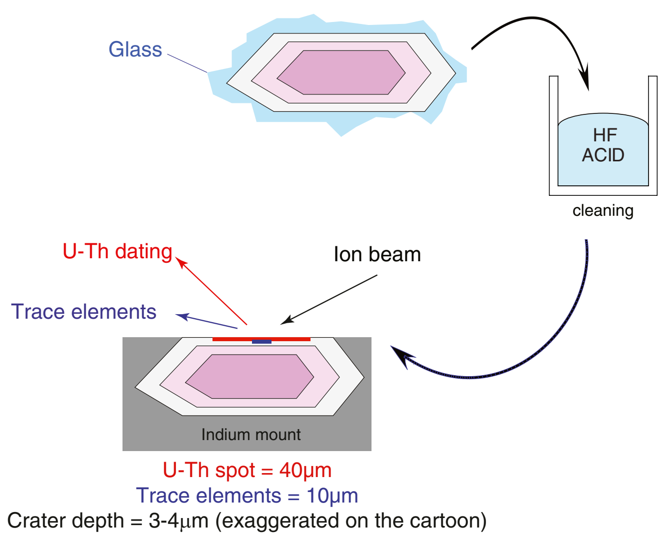

Fig. S3. Schematic sketch illustrating the technique for zircon dating and trace element analyses by SIMS used in this study.

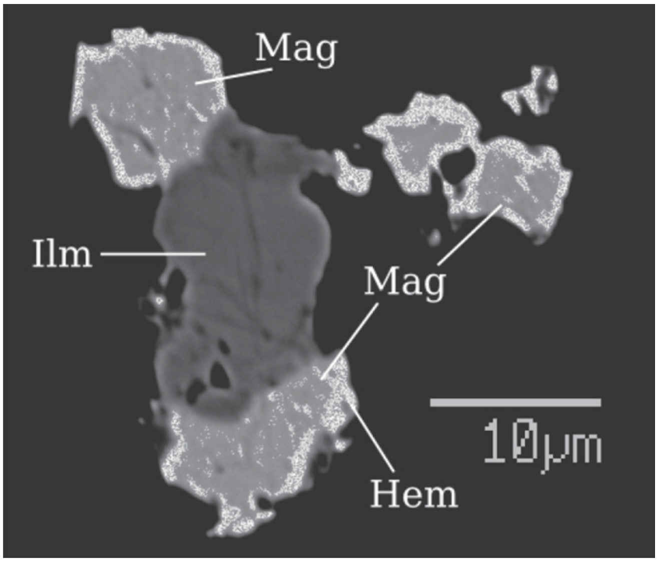

Fig. S4. SEM backscatter image from Terre Blanche SVC lava showing the coexisting Fe-Ti oxides used for the aTiO_2 determination (ilmenite, dark gray; magnetite, light gray; hematite rims, white; matrix, black).

Dataset S1. Whole-rock geochemistry

Dataset S1

Dataset S2. Zircon U-Th model ages and trace elements

Dataset S2

Dataset S3. ***a*TiO_2 calculation using the equilibrium between coexisting ilmenite and magnetite**

Dataset S3